Acta Crystallographica Section F
Structural Biology and Crystallization Communications
ISSN 1744-3091

Production and crystallization of the C-propeptide trimer from human procollagen III

J.-M. Bourhis,[a,b] N. Mariano,[a] Y. Zhao,[c] T. S. Walter,[c] K. El Omari,[c] F. Delolme,[d] C. Moali,[a] D. J. S. Hulmes[a]* and N. Aghajari[e]

[a]FRE 3310, Institut de Biologie et Chimie des Protéines, CNRS/Université Lyon 1, 69367 Lyon CEDEX 7, France, [b]Biologie Structurale des Interactions entre Virus et Cellule-Hôte, Université Joseph Fourier/European Molecular Biology Laboratory/CNRS UMI3265, 38042 Grenoble CEDEX 9, France, [c]Division of Structural Biology, Wellcome Trust Centre for Human Genetics, University of Oxford, Oxford OX3 7BN, England, [d]FR3302, Institut de Biologie et Chimie des Protéines, CNRS/Université Lyon 1, 69367 Lyon CEDEX 7, France, and [e]UMR5086, Institut de Biologie et Chimie des Protéines, CNRS/Université Lyon 1, 69367 Lyon CEDEX 7, France

Correspondence e-mail: d.hulmes@ibcp.fr

Received 20 July 2012
Accepted 9 August 2012

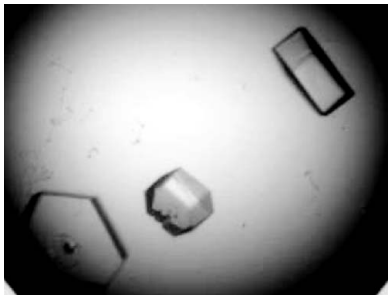

The C-propeptide domains of the fibrillar procollagens, which are present throughout the Metazoa in the form of ∼90 kDa trimers, play crucial roles in both intracellular molecular assembly and extracellular formation of collagen fibrils. The first crystallization of a C-propeptide domain, that from human procollagen III, is described. Following transient expression in mammalian 293T cells of both the native protein and a selenomethionine derivative, two crystal forms of the homotrimer were obtained: an orthorhombic form ($P2_12_12_1$) that diffracted to 1.7 Å resolution and a trigonal form ($P321$) that diffracted to 3.5 Å resolution. Characterization by MALDI-TOF mass spectrometry allowed the efficiency of selenomethionine incorporation to be determined.

1. Introduction

Fibrillar collagens (types I, II, III, V and XI) account for approximately 25% of protein mass in the body, where they occur in the form of banded fibrils with a characteristic 64–67 nm periodicity (Kadler *et al.*, 2007; Ricard-Blum, 2011). These collagens are synthesized in a precursor form, procollagen (∼450 kDa), as rod-like molecules (∼300 nm in length) with globular N- and C-terminal propeptide extensions (∼50 and 90 kDa, respectively). Each procollagen molecule consists of three polypeptide chains.

Inside the cell, procollagen molecular assembly is initiated by the trimerization of C-propeptide domains (Boudko *et al.*, 2011), followed by zipper-like folding towards the N-terminal end. Trimerization is a highly specific process leading to the correct association of chains into heterotrimers (procollagens I, V and XI) or homotrimers (procollagens I and II) and also preventing incorrect association of different genetic types. There is a region in the amino-acid sequence of the C-propeptide that controls specificity (Lees *et al.*, 1997), although the structural basis of chain recognition has yet to be elucidated. The importance of the C-propeptides in procollagen trimerization is underlined by the large number of heritable disorders of connective tissue that are characterized by mutations in this region of the molecule (Bateman *et al.*, 2009). These affect several tissues, including bone (Chessler *et al.*, 1993; Pace *et al.*, 2002), cartilage (Nishimura *et al.*, 2005), skin (De Paepe *et al.*, 1997) and blood vessels (Pickup & Pollanen, 2011).

Outside the cell (or during secretion), collagen fibril formation is triggered by proteolytic removal of the N- and C-terminal propeptides (Colige *et al.*, 2005; Kronenberg *et al.*, 2010; Muir & Greenspan, 2011; Vadon-Le Goff *et al.*, 2011) and is controlled by numerous interactions with other extracellular-matrix and cell-surface components (Kadler *et al.*, 2008). Solubility is assured by the presence of the propeptides, particularly the C-propeptides, which increase solubility by 1000-fold (Kadler *et al.*, 1987). The C-propeptides also interact with integrins (Davies *et al.*, 1997), with such interactions being involved in feedback regulation of biosynthesis (Mizuno *et al.*, 2000; Wu *et al.*, 1991) as well as angiogenesis and tumour progression (Palmieri *et al.*, 2008; Vincourt *et al.*, 2010). In addition, the C-propeptides are involved in mineralization (Kirsch & Pfäffle, 1992; Lee *et al.*, 1996; Lindahl *et al.*, 2011).

Despite their obvious biomedical importance, high-resolution three-dimensional structures of the fibrillar procollagen C-propeptides

Table 1
Crystallization conditions.

	Form I (SeMet)	Form II (native)	Form III (native)
Method	Sitting drop	Sitting drop	Sitting drop
Plate type	96-well Greiner	96-well Greiner	96-well Greiner
Temperature (K)	294	294	294
Protein concentration (mg ml^{-1})	30	30	30
Buffer composition of protein solution	20 m*M* HEPES pH 7.4, 0.15 *M* NaCl	20 m*M* HEPES pH 7.4, 0.15 *M* NaCl	20 m*M* HEPES pH 7.4, 0.15 *M* NaCl
Composition of reservoir solution	20% PEG 3350, 0.2 *M* NaCl	20% PEG 3350, 0.1 *M* bis-Tris propane pH 6.5, 0.2 *M* KNO_3	8% PEG 6000, 60 m*M* HEPES pH 7.0, 40 m*M* MES pH 6.0
Volume (nl) and ratio of drop	100, 1:1	100, 1:1	100, 1:1
Volume of reservoir (µl)	100	100	100

have thus far remained elusive. Low-resolution structural analysis of the C-propeptide trimer from procollagen III by small-angle X-ray scattering revealed a tri-lobed structure (Bernocco *et al.*, 2001), suggesting that the three polypeptide chains associate at their N-termini and then separate into distinct globular domains. This was reinforced by amino-acid sequence analysis, which identified a coiled-coil-like motif in this N-terminal region (McAlinden *et al.*, 2003). Relatively extended structures have also been proposed based on model building (Malone *et al.*, 2005). To gain further information, high-resolution structural data are clearly urgently required. Here, we describe the large-scale production, purification and crystallization of the C-propeptide trimer from human procollagen III in both native and selenomethionine-labelled forms, resulting in X-ray diffraction data to 1.7 Å resolution and thus heralding the first molecular structure determination for this important protein domain.

2. Methods

2.1. Expression and purification

DNA encoding the C-propeptide trimer from human procollagen III (CPIIIHis) was amplified from a previous construct in pBAC3 (Vadon-Le Goff *et al.*, 2011) using the forward primer 5′-ACCGGTCATCATCACCACCATCACTCC-3′ and the reverse primer 5′-TCTAGACTCGAGTTATAAAAAGCAAACAGG-3′ and then inserted into the *Age*I and *Xho*I sites of the pHLsec vector (Aricescu *et al.*, 2006). The corresponding protein is mutated at the single N-glycosylation site (N185Q) and contains an N-terminal His_6 tag followed by a Ser-Ala sequence just before the start of the native protein (Vadon-Le Goff *et al.*, 2011; see Fig. 1). Plasmid DNA was amplified in *Escherichia coli* XL1 Blue cells and then purified using the Endofree Plasmid Giga kit (Qiagen). For protein expression, mammalian HEK 293T cells were cultured in six 555 ml Hyperflasks (Corning) in a CompacT SelecT automated cell-culture system (TAP Biosystems) in DMEM (high glucose) supplemented with 1× non-essential amino acids (PAA) and 10% foetal bovine serum (FBS, Invitrogen). The cells were transfected at 90% confluence with DNA–PEI transfection mixture. This latter was prepared, for each Hyperflask, by pre-incubating 1 mg plasmid DNA with 2 mg branched polyethyleneimine (PEI MW 25 000; Aldrich) for 10 min at room temperature in 100 ml serum-free DMEM. After the DNA–PEI mixture was delivered into each Hyperflask, DMEM containing 2% FBS (455 ml) was used to top up the flask (Zhao *et al.*, 2011).

Figure 1
Amino-acid sequence of the expressed protein. The arrow indicates the start of the secreted protein after cleavage of the signal peptide. The His_6 sequence is shown in red and the arrowhead shows the start of the corresponding native protein after cleavage from procollagen by BMP-1 and tolloid-like proteinases. The Asn185Q mutation in the *N*-glycosylation site is boxed.

After 4 d, conditioned medium (3.3 l) was collected and was then clarified by centrifugation and filtration through a Steritop vacuum-driven filtration system (Millipore). The supernatant was then dialyzed over 2 d (with one change) against phosphate-buffered saline (PBS) at 277 K. Dialyzed medium was then applied onto a 5 ml column of Talon Co^{2+}-affinity resin (Clontech) followed by washing with four column volumes of phosphate-buffered saline (PBS) and two column volumes of PBS containing 20 m*M* imidazole. Bound protein was eluted with 250 m*M* imidazole in 20 m*M* Tris–HCl pH 8.0, 150 m*M* NaCl. Fractions were then pooled, microconcentrated (molecular-weight cutoff 30 kDa) and further purified on a Superdex 200 16/60 column eluted with 20 m*M* HEPES pH 7.4, 150 m*M* NaCl. Finally, fractions were analyzed by SDS–PAGE and further concentrated to ∼30 mg ml^{-1}.

For production of the selenomethionine derivative, cell culture and transfection were performed as above using 12 roller bottles (Greiner) instead of Hyperflasks. After 24–48 h transfection in normal DMEM containing 2% FCS (250 ml per roller bottle), the culture medium was removed, the cell layer was washed twice with PBS, and fresh methionine-free DMEM (MP Biomedicals) containing 3% dialyzed FBS medium was then added together with L-Gln, non-essential amino acids and 30 mg ml^{-1} L-selenomethionine (SeMet; Eburon Organics). After 4 d of culture, the medium was collected and the SeMet derivative was purified as for CPIIIHis (above).

2.2. Mass spectrometry

Mass spectrometry was performed using a Voyager-DE Pro MALDI-TOF mass spectrometer (Applied Biosystems) equipped with a nitrogen UV laser (λ = 337 nm, 3 ns pulse). The instrument was operated in the positive linear mode (mass accuracy 0.05%) with an accelerating potential of 20 kV. Typically, mass spectra were obtained by the accumulation of 600 laser shots for each analysis and were processed using *Data Explorer* 4.0 software (AB Sciex). For analysis of reduced proteins, 10 µl CPIIIHis and its SeMet derivative (at ∼3 mg ml^{-1}) were first reduced with 30 µl dithiothreitol (DTT; 10 m*M* in ammonium bicarbonate buffer) for 45 min at 328 K with constant stirring. After desalting using C4 ZipTips (Millipore), samples were mixed with sinapinic acid (saturated solution in 30% acetonitrile and 0.3% trifluoroacetic acid), deposited on the MALDI target and air-dried before analysis.

Table 2
Data collection and processing.

Values in parentheses are for the outer shell.

	Form I (SeMet)	Form II (native)	Form III (native)
Diamond beamline	I03	I04	I04
Wavelength (Å)	0.9795	0.9763	0.9763
Temperature (K)	100	100	100
Detector	ADSC Q315r	PILATUS 6M-F	PILATUS 6M-F
Crystal-to-detector distance (mm)	288	320	553
Rotation range per image (°)	1.0	0.1	0.1
Total rotation range (°)	360	360	360
Exposure time per image (°)	0.5	0.1	0.1
Space group	$P2_12_12_1$	$P2_12_12_1$	$P321$
Unit-cell parameters (Å, °)	a = 83.9, b = 89.3, c = 101.5, $\alpha = \beta = \gamma$ = 90	a = 76.5, b = 90.4, c = 102.4, $\alpha = \beta = \gamma$ = 90	$a = b$ = 86.1, c = 73.0, $\alpha = \beta$ = 90, γ = 120
Molecules in the asymmetric unit	3	3	1
Mosaicity (°)	0.40	0.75	1.61
Resolution range (Å)	101.5–2.2 (2.27–2.21)	61.3–1.7 (1.73–1.68)	43.0–3.5 (3.69–3.50)
Total No. of reflections	557946	271723	32977
No. of unique reflections	38676	78019	4149
Completeness (%)	100 (100)	96.2 (95.6)	99.7 (99.8)
Redundancy	14.4 (14.7)	3.5 (3.6)	7.9 (8.2)
Anomalous completeness (%)	100 (100)	n.a.	n.a.
Anomalous redundancy	7.6	n.a.	n.a.
$\langle I/\sigma(I)\rangle$	19.4 (4.0)	4.7 (2.2)	10.7 (3.2)
$R_{\rm r.i.m.}$ (%)	11.7	10.2	10.5
Overall B value from Wilson plot (Å^2)	34.9	21.5	93.6

2.3. Crystallization and data collection

Initial screening and optimization of crystallization conditions were carried out using a Cartesian Technologies pipetting robot in 96-well sitting-drop vapour-diffusion plates (Greiner). Crystallization kits from Hampton Research (Index and SaltRx), Molecular Dimensions (PACTpremier) and the Oxford Protein Production Facility (Blocks 1–3; http://www.oppf.ox.ac.uk) were used. Crystals of forms I (SeMet) and II (native) were obtained directly using the Block 3 and PACTpremier crystallization kits, respectively, as detailed in Table 1. Crystals of form III (native) were initially obtained using the Block 3 kit in 10% PEG 6000, 0.1 *M* MES pH 6.0 and were optimized to the conditions shown in Table 1. Images of crystallization drops were taken automatically at regular intervals using a TAP Biosystems storage vault (Walter *et al.*, 2005) maintained at 294 K. Further information is provided in Table 1.

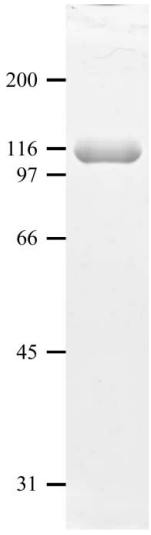

Figure 2
SDS–PAGE analysis. 5 µg purified CPIIIHis was analyzed on a 10% acrylamide gel under nonreducing conditions followed by Coomassie Blue staining. Migration positions of marker proteins are indicated in kDa.

For data collection, crystals were flash-cooled in liquid nitrogen. Form I crystals were cryoprotected by gradually increasing the glycerol concentration in the mother liquor to 30%(*v*/*v*), form II crystals were immersed in oil (perfluoropolyether PFO-X125/03; Alfa Aesar) and form III crystals were cryoprotected with 25% ethylene glycol. Diffraction data were collected at the Diamond Light Source synchrotron (Didcot, England). Data were processed using *xia*2 (form I) and *MOSFLM* (forms II and III) and were scaled with *SCALA* from the *CCP*4 program suite (Winn *et al.*, 2011). Each data set was collected from a single crystal. Data-collection and processing statistics are given in Table 2.

3. Results and discussion

Recombinant C-propeptide trimer from human procollagen III (CPIIIHis; where each chain is mutated at the single N-glycosylation site and carries an N-terminal His_6 tag; Vadon-Le Goff *et al.*, 2011) was expressed by large-scale transient transfection in HEK 293T cells (Aricescu *et al.*, 2006). Approximately 18 mg CPIIIHis was obtained from 3 l conditioned medium. Purity was at least 99% as assessed by SDS–PAGE (Fig. 2), which showed a single band (under nonreducing conditions) migrating at approximately the mass expected for a trimer. We also checked for purity and trimerization ability by mass spectrometry under both reducing and nonreducing conditions. By MALDI-TOF, the $[M + H]^+$ ion for trimeric CPIIIHis was observed at an m/z value of 86 403 ± 43 (Fig. 3*a*). After reduction with DTT, the $[M + H]^+$ ion for monomeric CPIIIHis was observed at m/z = 28 769 ± 14 (Fig. 3*b*). These figures compared favourably with the expected molecular masses of 86 320 and 28 776 Da, respectively. Thus, both the SDS–PAGE and the mass-spectrometric data showed that the presence of the N-terminal His_6 tag did not interfere with the trimerization of CPIIIHis.

For structure determination, as there are no homologues of the fibrillar procollagen C-propeptides in the Protein Data Bank, heavy-atom labelling or selenium substitution is required in order to solve the phase problem. Since the transient expression system used here has previously been shown to efficiently incorporate free seleno-methionine from the culture medium (Aricescu *et al.*, 2006), we also

produced the SeMet derivative of CPIIIHis (see §2), resulting in good, although somewhat reduced, yields (∼6 mg).

Analysis of the SeMet derivative of CPIIIHis by MALDI-TOF mass spectrometry showed a minor $[M + H]^+$ ion signal at m/z = 28 773 ± 14 and a broader major $[M + H]^+$ ion signal at m/z = 29 023 ± 15 (Fig. 3*c*). The first peak corresponds to unlabelled monomer (representing ∼25% of the total), while the broader peak (∼75% of the total) indicates a mixed population of selenomethionine-labelled protein species with an average mass corresponding to approximately five selenomethionine residues incorporated into each CPIIIHis monomer (the mass increment per SeMet residue is 47). This compares with six methionine residues per chain observed in the amino-acid sequence of CPIIIHis. The incorporation of the SeMet label into CPIIIHis was therefore highly efficient.

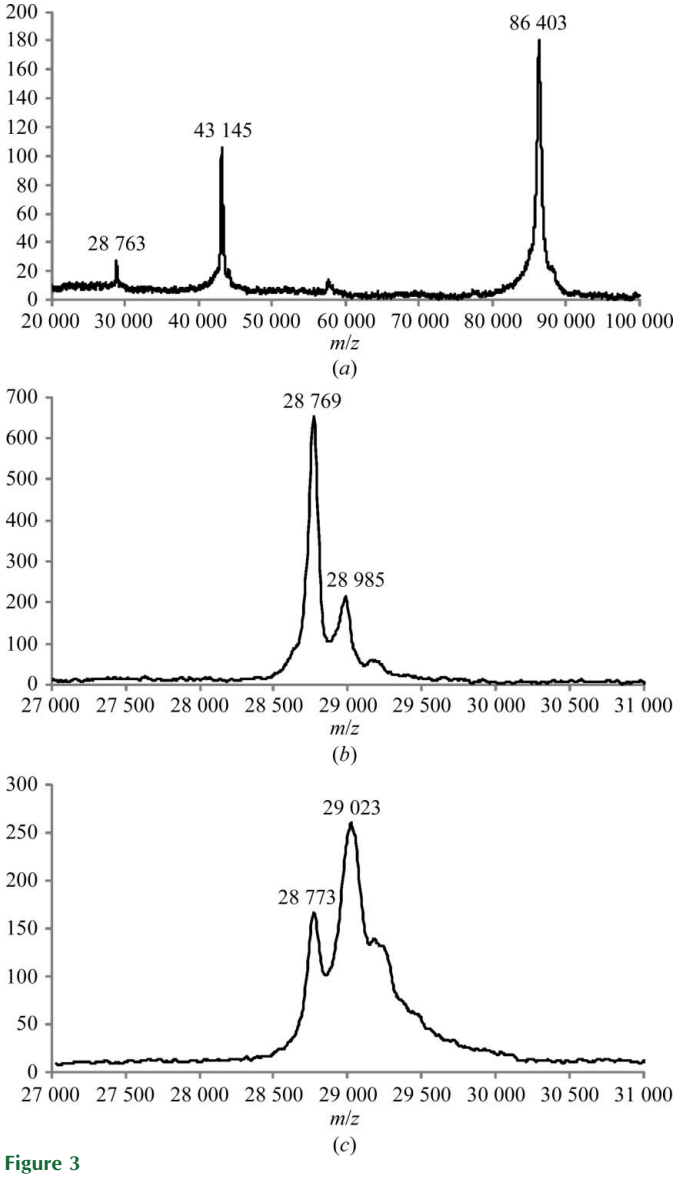

Figure 3
Mass-spectrometric analysis. (*a*) MALDI-TOF spectrum of nonreduced CPIIIHis showing the major singly charged $[M + H]^+$ ion at m/z = 86 403 as expected for the trimer, as well as doubly $[M + 2H]^{2+}$ and triply $[M + 3H]^{3+}$ charged ions at m/z = 43 145 and 28 763, respectively. (*b*) MALDI-TOF spectrum of reduced CPIIIHis showing a major peak at m/z = 28 769 as expected for the monomeric form. The minor $[M + H]^+$ ion at m/z = 28 985 probably corresponds to a noncovalent adduct with one molecule of sinapinic acid matrix. (*c*) MALDI-TOF spectrum of the CPIIIHis SeMet derivative showing a major $[M + H]^+$ ion at m/z = 29 023 corresponding to the incorporation of approximately five SeMet residues per monomer. The minor $[M + H]^+$ ion at m/z = 28 773 corresponds to unlabelled CPIIIHis.

After concentration to approximately 30 mg ml^{-1}, crystallization trials were set up for the unlabelled and SeMet-labelled proteins. After a few days, crystals began to appear in several conditions (Table 1). In general, the crystals were of two types: needle-like

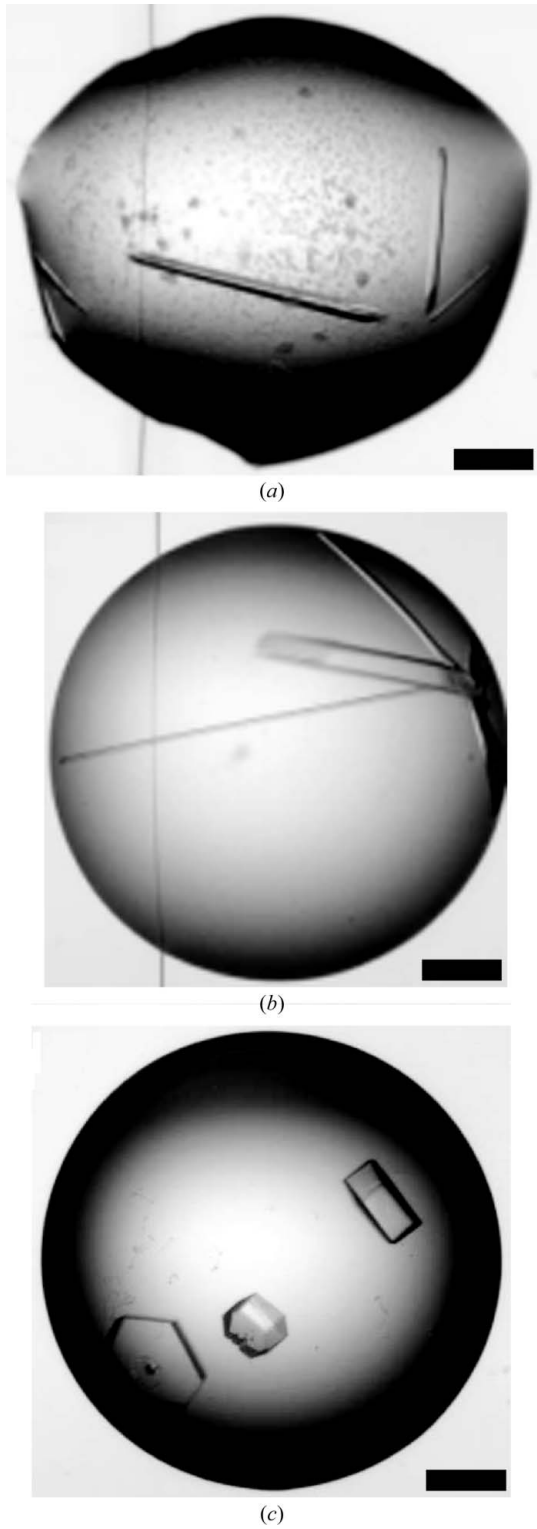

Figure 4
Crystallization. Crystals of the SeMet derivative of CPIIIHis (form I) are shown (*a*) as well as those of the two native forms II (*b*) and III (*c*). Scale bars = 200 µm.

or hexagonal plates (Fig. 4). X-ray diffraction screening of crystals grown under different conditions resulted in the identification of two crystal forms that diffracted X-rays to 1.7 and 3.5 Å resolution in space groups $P2_12_12_1$ and $P321$, respectively (Table 2). For the SeMet derivative, screening using the most promising conditions identified for the unlabelled protein also rapidly resulted in high-quality crystals (space group $P2_12_12_1$). These diffracted to 2.2 Å resolution and the anomalous signal in the data collected allowed phasing to be carried out. Structure determination using single-wavelength anomalous dispersion is described elsewhere (Bourhis *et al.*, 2012).

This work was funded by the Fondation de France, the Agence National de la Recherche (SCARFREE and TOLLREG projects), the European Commission (P-CUBE project), the Centre National de la Recherche Scientifique, the Université Lyon 1 and Lyinbiopôle. We thank Annie Chaboud and Isabelle Grosjean of the Protein Production and Analysis Facility (SFR Biosciences Gerland-Lyon Sud UMS3444/US8) as well as the staff of Diamond Light Source (Didcot, England) for technical support.

References

Aricescu, A. R., Lu, W. & Jones, E. Y. (2006). *Acta Cryst.* D**62**, 1243–1250.
Bateman, J. F., Boot-Handford, R. P. & Lamandé, S. R. (2009). *Nature Rev. Genet.* **10**, 173–183.
Bernocco, S., Finet, S., Ebel, C., Eichenberger, D., Mazzorana, M., Farjanel, J. & Hulmes, D. J. S. (2001). *J. Biol. Chem.* **276**, 48930–48936.
Boudko, S. P., Engel, J. & Bachinger, H. P. (2011). *Int. J. Biochem. Cell Biol.* **44**, 21–32.
Bourhis, J.-M., Marinaro, N., Zhao, Y., Harlos, K., Exposito, J.-Y., Jones, E. Y., Moali, C., Aghajari, N. & Hulmes, D. J. S. (2012). *Nature Struct. Mol. Biol*. In the press.
Chessler, S. D., Wallis, G. A. & Byers, P. H. (1993). *J. Biol. Chem.* **268**, 18218–18225.
Colige, A., Ruggiero, F., Vandenberghe, I., Dubail, J., Kesteloot, F., Van Beeumen, J., Beschin, A., Brys, L., Lapière, C. M. & Nusgens, B. (2005). *J. Biol. Chem.* **280**, 34397–34408.
Davies, D., Tuckwell, D. S., Calderwood, D. A., Weston, S. A., Takigawa, M. & Humphries, M. J. (1997). *Eur. J. Biochem.* **246**, 274–282.
De Paepe, A., Nuytinck, L., Hausser, I., Anton-Lamprecht, I. & Naeyaert, J. M. (1997). *Am. J. Hum. Genet.* **60**, 547–554.
Kadler, K. E., Baldock, C., Bella, J. & Boot-Handford, R. P. (2007). *J. Cell Sci.* **120**, 1955–1958.
Kadler, K. E., Hill, A. & Canty-Laird, E. G. (2008). *Curr. Opin. Cell Biol.* **20**, 495–501.
Kadler, K. E., Hojima, Y. & Prockop, D. J. (1987). *J. Biol. Chem.* **262**, 15696–15701.
Kirsch, T. & Pfäffle, M. (1992). *FEBS Lett.* **310**, 143–147.
Kronenberg, D., Bruns, B. C., Moali, C., Vadon-Le Goff, S., Sterchi, E. E., Traupe, H., Böhm, M., Hulmes, D. J. S., Stöcker, W. & Becker-Pauly, C. (2010). *J. Invest. Dermatol.* **130**, 2727–2735.
Lee, E. R., Smith, C. E. & Poole, R. (1996). *J. Histochem. Cytochem.* **44**, 433–443.
Lees, J. F., Tasab, M. & Bulleid, N. J. (1997). *EMBO J.* **16**, 908–916.
Lindahl, K. *et al.* (2011). *Hum. Mutat.* **32**, 598–609.
Malone, J. P., Alvares, K. & Veis, A. (2005). *Biochemistry*, **44**, 15269–1 5279.
McAlinden, A., Smith, T. A., Sandell, L. J., Ficheux, D., Parry, D. A. & Hulmes, D. J. S. (2003). *J. Biol. Chem.* **278**, 42200–42207.
Mizuno, M., Fujisawa, R. & Kuboki, Y. (2000). *Calcif. Tissue Int.* **67**, 391–399.
Muir, A. & Greenspan, D. S. (2011). *J. Biol. Chem.* **286**, 41905–41911.
Nishimura, G., Haga, N., Kitoh, H., Tanaka, Y., Sonoda, T., Kitamura, M., Shirahama, S., Itoh, T., Nakashima, E., Ohashi, H. & Ikegawa, S. (2005). *Hum. Mutat.* **26**, 36–43.
Pace, J. M., Chitayat, D., Atkinson, M., Wilcox, W. R., Schwarze, U. & Byers, P. H. (2002). *J. Med. Genet.* **39**, 23–29.
Palmieri, D., Astigiano, S., Barbieri, O., Ferrari, N., Marchisio, S., Ulivi, V., Volta, C. & Manduca, P. (2008). *Exp. Cell Res.* **314**, 2289–2298.
Pickup, M. J. & Pollanen, M. S. (2011). *Forensic Sci. Med. Pathol.* **7**, 192–197.
Ricard-Blum, S. (2011). *Cold Spring Harb. Perspect. Biol.* **3**, a004978.
Vadon-Le Goff, S., Kronenberg, D., Bourhis, J.-M., Bijakowski, C., Raynal, N., Ruggiero, F., Farndale, R. W., Stöcker, W., Hulmes, D. J. S. & Moali, C. (2011). *J. Biol. Chem.* **286**, 38932–38938.
Vincourt, J.-B., Etienne, S., Cottet, J., Delaunay, C., Malanda, C. B., Malanda, B., Lionneton, F., Sirveaux, F., Netter, P., Plénat, F., Mainard, D., Vignaud, J.-M. & Magdalou, J. (2010). *Cancer Res.* **70**, 4739–4748.
Walter, T. S. *et al.* (2005). *Acta Cryst.* D**61**, 651–657.
Winn, M. D. *et al.* (2011). *Acta Cryst.* D**67**, 235–242.
Wu, C. H., Walton, C. M. & Wu, G. Y. (1991). *J. Biol. Chem.* **266**, 2983–2987.
Zhao, Y., Bishop, B., Clay, J. E., Lu, W., Jones, M., Daenke, S., Siebold, C., Stuart, D. I., Jones, E. Y. & Aricescu, A. R. (2011). *J. Struct. Biol.* **175**, 209–215.